IEEE Access
Multidisciplinary | Rapid Review | Open Access Journal

Received September 30, 2019, accepted October 25, 2019, date of publication October 31, 2019,
date of current version November 13, 2019.

Digital Object Identifier 10.1109/ACCESS.2019.2950683

Uncertainty Analysis for Characterization of a Commercial Real-Time Oscilloscope Using a Calibrated Pulse Standard

CHIHYUN CHO, (Member, IEEE), HYUNJI KOO, (Member, IEEE), JAE-YONG KWON, (Senior Member, IEEE), AND JOO-GWANG LEE, (Member, IEEE)

Center for Electromagnetic Metrology, Division of Physical Metrology, Korea Research Institute of Standards and Science, Daejeon 305-340, South Korea

Corresponding author: Chihyun Cho (chihyun.cho@kriss.re.kr)

This work was supported by the Physical Metrology for National Strategic Needs funded by the Korea Research Institute of Standards and Science under Grant KRISS-2019-GP2019-0005.

ABSTRACT In this paper, we describe a traceable measurement method for the frequency response of commercial real-time digital oscilloscopes (RTDOs). Since the commercial RTDOs usually use multiple analog digital convertors (ADCs), it is very challenging to characterize each ADC without having access to the internal circuitry. In this study, we use an additional continuous wave (CW) source to match the sampling sequence in a time interleaved ADC (TIADC). We also use a calibrated pulse standard traceable to the National Institute of Standards and Technology (NIST). Since the sampling rate of a single ADC is greatly reduced, we slightly misalign the sampling rate of the pulse and the single ADC and then stack the multiple measured pulses as a single pulse. As a result, the sampling rate can be greatly increased by about 8000 times. The frequency response of the RTDO during testing shows a variation of ± 1 dB in amplitude and $\pm 7^\circ$ in phase between ADCs at the maximum operating frequency. These differences need to be calibrated as they cause systematic errors in the measurement. The 95% confidence interval of the measured frequency response is about 0.2 dB in amplitude and 3° in phase. Finally, the measured amplitude is compared with the swept sine measurement method, which confirms that they agree well within its uncertainties.

INDEX TERMS Oscilloscopes, real time systems, calibration, frequency response, metrology, measurement uncertainty.

I. INTRODUCTION

Recently a commercial real-time oscilloscope (RTDO) has been widely used in various applications because the bandwidth and sampling rate have greatly increased. This apparatus usually employs a time interleaved analog digital convertor (TIADC) architecture that is a sequential sampling technique using multiple ADCs. Thus, each ADC is required to have the same characteristics. However, they cannot be completely identical due to the manufacturing process or design. The difference between these ADCs causes systematic errors inherent in the TIADC architecture [1].

In the past, the bandwidth of most RTDOs was sub-GHz, and this impairment in the TIADC could be represented as offset error, gain, and timing skew. Various studies have been carried out to correct these static errors. However, as the bandwidth of the RTDO has increased, these errors can no longer be regarded as static, and they clearly change depending on frequency, which makes it more difficult to calibrate.

A method was proposed for evaluating the relative difference of the TIADC using a continuous wave (CW) source [2], [3]. They showed that the frequency-dependent difference can be modeled as a frequency response and offset errors. They also proved that the input signal can be perfectly reconstructed with the prior known frequency response of each ADC when the input signal is band-limited. This method can not provide traceability in the phase relationship between ADCs. In [4], the frequency response of each ADC was measured with the traceability on both the amplitude and the phase by applying the calibrated pulse. However, the measurement uncertainty was not provided.

In a previous paper, we improved the accuracy of aligning the measured pulses and matching the frequency grid [5]. In this paper we describe the method explained in [5] in more

The associate editor coordinating the review of this manuscript and approving it for publication was Wei Liu.

detail and fully analyze the measurement uncertainty of the proposed method. As far as we know, this is the first study to analyze the measurement uncertainty of the frequency response for the commercial RTDO. The measurement uncertainty is also verified by a comparison with the swept sine method.

This paper is organized as follows. Section II reviews the measurement method for the frequency response of the TIADC in the commercial RTDO. In Section III, a detailed analysis of the uncertainties for the measurement method is described. Section IV concludes the paper.

II. CHARACTERIZATION METHOD

In order to measure the frequency response of an individual ADC for a commercial RTDO, some prior information is required. We need to know the number of ADCs used in the apparatus and match the sequence of ADCs that change in each measurement. A detailed description can be found in [2], [3].

A. MEASUREMENT SETUP

The measurement setup to characterize the frequency response of the commercial RTDO is shown in Fig. 1. In this study, a photodiode (PD) calibrated from the National Institute of Standards and Technology (NIST) was used as the pulse standard. The voltage source supplied 2V to the PD, and it simultaneously monitored the current consumed on the PD. The RTDO and the PD were connected through the adapter because the PD had a 1.0 mm coaxial output while the RTDO had 3.5 mm. The femtosecond laser source with 1550 nm was used to derive the PD, and the laser synchronization unit (laser sync. unit) was adapted to precisely control the repetition rate of the laser source. The additional RF source with 3.3 GHz was applied to another channel of the RTDO to match the sequence of the TIADC.

At NIST, the calibration was done at the end of an optical cable that was attached to a PD of about 1 m. The additional cable produced results different from the calibration data from NIST due to the dispersion effect. In this study, we attached the focus lens at the output of the laser source to connect the PD. It was also possible to adjust the intensity of the optical signal to be coupled to the PD by adjusting the focus of the lens. It is known that 1 ps of dispersion typically occurs per 1 meter of optical cable. This length produces approximately 0.02 dB of additional attenuation at 25 GHz. It is also known that very few dispersions occur with very thin focus lenses of several mm. Thus we could assume that there was no additional dispersion effect on the measurement.

B. SUPERIMPOSING PULSE

The measurement of the pulse needs to be separated with respect to ADCs to obtain the frequency response of each ADC. As a result, the sampling rate is reduced by the number of ADCs in the TIADC. If the repetition rate of the laser source is slightly changed so as not to match the pulse train and the sampling point, the sampling rate can be greatly increased by stacking the pulse train on a single pulse [4].

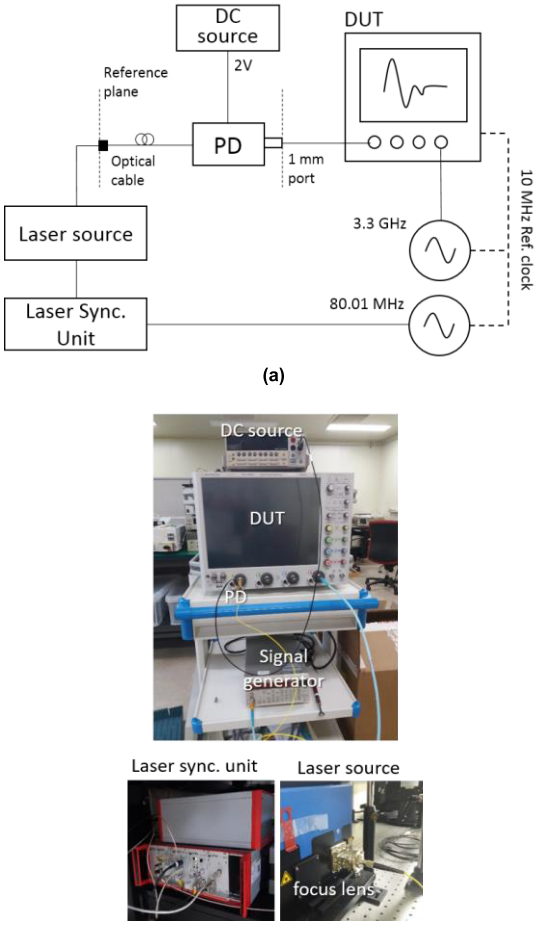

FIGURE 1. Measurement setup for characterizing the frequency response of a commercial RTDO (a) block diagram (b) photos.

In this study, the RTDO had a sampling rate of 80 GS/s with 320 ADCs per channels. Thus the separate data depending on each ADC greatly reduced the sampling rate to 250 MHz. We set the repetition rate of the laser sync. unit at 80.01 MHz. Then the measured pulse train was cut with the repetition rate of the laser source, and they overlapped as a single pulse. When the measurement was performed for $t_{uniform}$ second, the superimposed data had the same time interval between all the samples.

$$t_{uniform} = \frac{1}{\gcd(F_S, F_R)}$$

where gcd is the greatest common divisor, F_S is the sampling rate of a single ADC, and F_R is the repetition rate of the laser source. Thus, the superimposed pulse increased the sampling rate to $F_{S\_up} = 2.0025$ TS/s, calculated as

$$F_{S\_up} = t_{uniform} F_S F_R$$

C. PULSE ALIGNMENT

The RTDO has large noise compared to other types of oscilloscope because it usually employs a low ADC bit (8-10 bit) to capture fast signals in real time. The noise source of the oscilloscope is ADC quantization noise, ADC differential nonlinearity, ADC integral nonlinearity, thermal noise, shot noise and input amplifier distortion, etc. Averaging reduces the thermal noise as well as other noise sources, which is equivalent to increasing the number of bits. Thus, the averaging process is essential to reducing the noise of the RTDO. Before the averaging process, the measured pulses need to be precisely aligned to each other. One way to delay the measurement signal by Δt is to multiply the Fourier transformed signal by $\exp(-j\omega\Delta t)$. Thus, the alignment process can be expressed as

$$\min\left(\sum_{k=1}^{N} V_{ref}(f_k) - V_{mov}(f_k)e^{-j\omega_k\Delta t}\right) \tag{1}$$

where ω is the angular frequency and $V_{ref}(f)V_{mov}(f)$ are the Fourier transform of the reference pulse and alignment pulse, respectively. If we only consider the phase, (1) can be represented as a linear form as follows:

$$\min\left(\sum_{k=1}^{N} \phi_{ref}(f_k) - \phi_{mov}(f_k) + \omega_k\Delta t\right) \tag{2}$$

In other words, the time delay Δt is a value that minimizes the difference between the phase of the reference and alignment pulses. Thus, it can be considered as a linear fitting problem, and can be expressed as follows:

$$\Delta t = -\boldsymbol{\omega}^{-1}(\boldsymbol{\Phi}_{ref} - \boldsymbol{\Phi}_{mov}) \tag{3}$$

$$V_{scope}(f) = V_{mov}(f)e^{-j\omega\Delta t} \tag{4}$$

where $\boldsymbol{\omega} = [\omega_0, \omega_1, \ldots, \omega_N]'$ and $\boldsymbol{\Phi} = [\phi(\omega_0), \phi(\omega_1), \ldots, \phi(\omega_N)]'$ are the angular frequency and unwrapped phase, and $'$ is the transpose. Then the aligned pulses V_{scope} are again transformed to the time domain after the value Δt is added [5]. The reference pulse may be selected arbitrarily from the set of measurement pulses, and the remains of the measurements become alignment pulses. In this study, we set ω_N to $2\pi \times 25$ GHz, which is the maximum operating frequency of the RTDO during testing.

Fig. 2 shows the alignment of 100 measured pulses and their standard deviations (dotted line). The standard deviations are not so different because they are well aligned with each other. In the rising and falling time interval of the pulses (about 2.26 ns and 2.29 ns), the standard deviation slightly increases due to the random jitter of the ADC. The effect of the jitter can be calculated as [6]

$$\sigma_{pulse}^2 = \sigma_{noise}^2 + \left(\frac{\partial v_{scope}(t)}{\partial t}\right)^2\sigma_{jitter}^2 \tag{5}$$

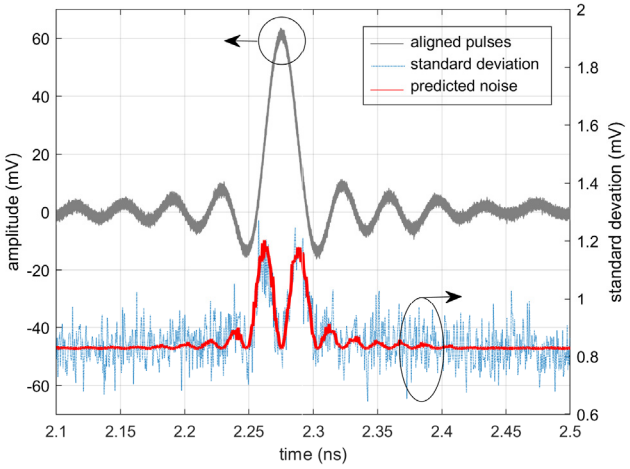

FIGURE 2. Aligning measured pulses and their standard deviation.

where σ_{noise} and σ_{jitter} are the standard deviation of the random noise and random jitter for each ADC, respectively. $v_{scope}(t)$ is the measurement pulse, and σ_{pulse} is the standard deviation of the pulse due to the noise and jitter.

Thus, the random jitter can be predicted with the measured $\sigma_{noise} = 827.5\ \mu$V and (5). The estimated jitter is about 200 fs and the predicted value is shown in Fig. 2 with the thick solid line. The predicted result is in good agreement with the standard deviation of the measured values, which is then used in the analysis of the measurement uncertainty. Note that the output voltage noise of the PD and the noise floor of the RTDO are indistinguishable. Likewise, the jitter of the ADC in the RTDO and the jitter of the femtosecond laser can not be distinguished.

D. FREQUENCY GRID ALIGNMENT

The voltage response of the PD had a 200 MHz interval, whereas the measured pulses of the RTDO had a frequency grid of 80.01 MHz. Thus, the measured pulses were linearly interpolated to 2 TS/s from the sampling rate of 2.00025 TS/s in the time domain. The interpolated data then had a total measurement time of 12.5 ns. The measurement time was adjusted to 10 ns by a truncating 2.5 ns section in which only the noise was measured. Then, the data had a 100 MHz grid in the frequency domain, so it easily matched the PD data with a frequency grid of 200 MHz.

E. CALIBRATION OF IMPEDANCE MISMATCH

An adapter was used to connect the 1 mm output port of the PD and the 3.5 mm input port of the RTDO. The impedance mismatch between them can be calibrated [7] as in (6), as shown at the bottom of this page, where H is the frequency

$$H = \frac{V_{scope}\left(1 - \Gamma_{PD}S_{11} - \Gamma_{scope}S_{22} - \Gamma_{PD}\Gamma_{scope}(S_{21}S_{12} - S_{11}S_{22})\right)}{V_{PD}S_{21}} \tag{6}$$

response of the RTDO, V_{SCOPE} and V_{PD} are the measured pulse using the RTDO and the voltage response of the calibrated PD where both are in the frequency domain. Γ_{scope} and Γ_{PD} are the reflection coefficients of the RTDO and the PD, and S_{xx} is the S parameters of the adapter. The impedance of the adapter, source, and PD was measured using a vector network analyzer (VNA), and the measurement uncertainty was analyzed based on the physical parameters [8], [9]. Therefore, the full covariance between not only real and imaginary values but also all frequency values can be obtained and it can be converted from the frequency domain to the time domain and vice versa [10]. Fig. 3 compares the frequency response of the RTDO before and after correction of the impedance mismatch. The frequency response improved by approximately 0.25 dB at 25 GHz.

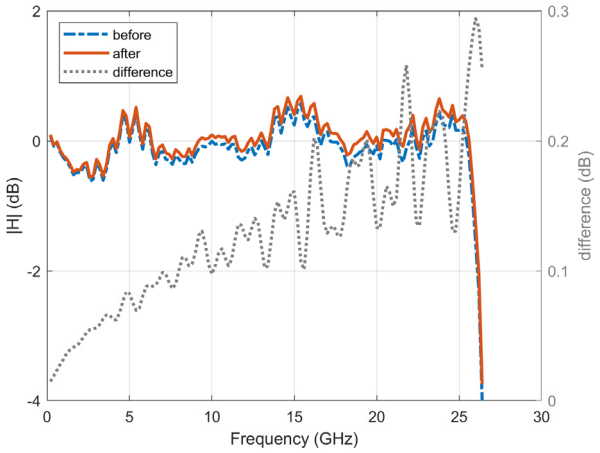

FIGURE 3. Impedance mismatch calibration result.

The characterized frequency responses of the RTDO during testing are shown in Fig. 4. The RTDO used in the measurement has 320 ADCs per channel. The amplitude varies by about ± 1 dB and the phase changes by about ± 7 ° at the maximum operating frequency of 25 GHz. The difference between ADCs generates many spur and aliasing signals in the measurement, making accurate measurement difficult. Therefore, the frequency response of each ADC needs to be precisely characterized, and these differences among the TIADCs needs to be calibrated.

III. UNCERTAINTY ANALYSIS

This section analyzes the measurement uncertainty of the proposed method. The main factors of uncertainty are the measured pulse using the RTDO, the impedance mismatch correction and the voltage response of the calibrated PD as shown in (6). The uncertainty for each term is as follows:

A. UNCERTAINTY OF THE MEASURED PULSE USING THE RTDO

The uncertainty of the measured pulse was due to inaccurate alignment and jitter noise. The estimation of the delay time

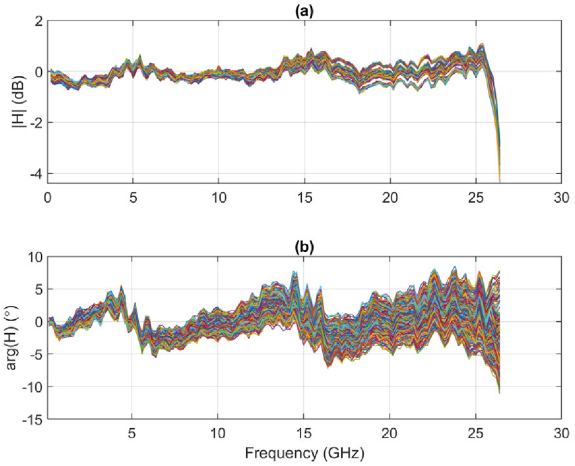

FIGURE 4. Frequency response of TIADCs. (from [5]).

Δt in (3) is a linear least square (LSQ) fitting procedure. Thus, the covariance of the delay time $\Sigma_{\Delta t}$ can be calculated from the LSQ fitting residual $\sigma_{residual}$ [11].

$$\mathbf{\Sigma}_{\Delta t} = \left(\mathbf{J}'_{fit}\mathbf{J}_{fit}\right)^{-1}\sigma_{residual}, \tag{7}$$

where $\mathbf{J}_{fit}$ is the Jacobean matrix with

$$\mathbf{J}_{fit} = \left[\frac{\partial(\phi_{ref}(\omega_0)-\tilde{\phi}_{PD}(\omega_0))}{\partial\Delta t} \cdots \frac{\partial(\phi_{ref}(\omega_N)-\tilde{\phi}_{PD}(\omega_N))}{\partial\Delta t}\right]'. \tag{8}$$

where $\tilde{\phi}_{PD}(\omega_0)$ is the phase of the averaged pulse $\tilde{v}_{scope}$ on ω_0. The uncertainty propagation of the correlated multivariables can be expressed by a first order Taylor approximation [12].

$$\begin{aligned} y &= f(x_1, \ldots, x_K) \\ \sigma_y^2 &= \sum_{i=1}^{K}\left(\frac{\partial f}{\partial x_i}\right)^2\sigma_{x_i}^2 + 2\sum_{i=1}^{K-1}\sum_{j=i+1}^{K}\frac{\partial f}{\partial x_i}\frac{\partial f}{\partial x_j}\sigma_{x_i x_j} \end{aligned} \tag{9}$$

where σ represents the standard deviation of the variables. Generalizing (9) to the matrix form can be expressed as the product of the Jacobian matrix and the covariance matrix [13]. Thus $\mathbf{\Sigma}_{\Delta t}$ is propagated to the covariance of the measured pulse $\mathbf{\Sigma}_{align}$ as follows:

$$\mathbf{\Sigma}_{align} = \mathbf{J}_{align}\mathbf{\Sigma}_{\Delta t}\mathbf{J}'_{align}, \tag{10}$$

where $\mathbf{J}_{align}$ is the Jacobian matrix for the sensitivity of the pulse amplitude to the delay time Δt.

$$\mathbf{J}_{align} = \left[\frac{\partial\tilde{v}_{scope}(t_0)}{\partial\Delta t} \quad \cdots \quad \frac{\partial\tilde{v}_{scope}(t_L)}{\partial\Delta t}\right]' \tag{11}$$

In (11), $\tilde{v}_{scope}(t)$ is the averaged pulse on t, and L is the length of the pulse. Next, the covariance $\mathbf{\Sigma}_{noise}$ for the random noise σ_{noise} and jitter σ_{jitter} on ADC is obtained by making a

diagonal matrix using (5) because the noise and the jitter have independent normal distribution.

$$\begin{aligned}\boldsymbol{\Sigma}_{noise} &= \begin{bmatrix} \sigma^2_{puse}(t_1) & 0 & 0 \\ 0 & \ddots & 0 \\ 0 & 0 & \sigma^2_{pulse}(t_L) \end{bmatrix} \\ &= \begin{bmatrix} \sigma^2_{noise} + \dfrac{\partial \tilde{v}_{PD}(t_1)}{\partial t_1}\sigma^2_{jitter} & 0 & 0 \\ 0 & \ddots & 0 \\ 0 & 0 & \sigma^2_{noise} + \dfrac{\partial \tilde{v}_{PD}(t_L)}{\partial t_L}\sigma^2_{jitter} \end{bmatrix}\end{aligned}$$

Then applying the central limit theorem, the covariance $\tilde{\boldsymbol{\Sigma}}_{noise}$ of the average pulse is obtained by dividing the covariance $\boldsymbol{\Sigma}_{noise}$ with the number of measurements N.

$$\tilde{\boldsymbol{\Sigma}}_{noise} = \boldsymbol{\Sigma}_{noise}/N$$

For the DUT used this work, $\sqrt{\tilde{\boldsymbol{\Sigma}}_{noise}}$ is about six times greater than $\sqrt{\boldsymbol{\Sigma}_{align}}$ on the rising and falling time of the measured pulse. To reduce covariance $\boldsymbol{\Sigma}_{noise}$, we increase the number of averaging or use an apparatus with a small quantized error.

Finally, the alignment covariance $\boldsymbol{\Sigma}_{align}$ and the noise covariance $\tilde{\boldsymbol{\Sigma}}_{noise}$ are propagated to the covariance $\boldsymbol{\Sigma}_{scope}$ for the frequency response using a Jacobian matrix $\mathbf{J}_{scope}$.

$$\boldsymbol{\Sigma}_{scope} = \boldsymbol{J}_{scope}(\boldsymbol{\Sigma}_{align} + \tilde{\boldsymbol{\Sigma}}_{noise})\boldsymbol{J}'_{scope} \tag{12}$$

$\mathbf{J}_{scope}$, which includes the frequency alignment process described in II-*D*, can be obtained based on (6) as follows:

$$\mathbf{J}_{scopoe} = \begin{bmatrix} \dfrac{\partial |H(f_0)|}{\partial v_{scope}(t_0)} & \cdots & \dfrac{\partial |H(f_0)|}{\partial v_{scope}(t_L)} \\ \vdots & & \vdots \\ \dfrac{\partial |H(f_M)|}{\partial v_{scope}(t_0)} & \cdots & \dfrac{\partial |H(f_M)|}{\partial v_{scope}(t_L)} \\ \dfrac{\partial \arg(H(f_0))}{\partial v_{scope}(t_0)} & \cdots & \dfrac{\partial \arg(H(f_0))}{\partial v_{scope}(t_L)} \\ \vdots & & \vdots \\ \dfrac{\partial \arg(H(f_M))}{\partial v_{scope}(t_0)} & \cdots & \dfrac{\partial \arg(H(f_M))}{\partial v_{scope}(t_L)} \end{bmatrix} \tag{13}$$

Note that arg(·) is the phase of (·), L is the length of the measured pulse, and M is the number of the frequency responses of the ADC. In this study, the complex frequency responses are expressed in terms of amplitude and phase, but the Jacobian matrix can be composed of real and imaginary terms as needed.

B. UNCERTAINTY OF IMPEDANCE MISMATCH AND RESPONSE OF PD

The impedance mismatch between the PD, RTDO, and adapter was calibrated using (6). Let the covariances of Γ_{scope}, Γ_{PD}, and S_{xx} be $\boldsymbol{\Sigma}_{\Gamma scope}$, $\boldsymbol{\Sigma}_{\Gamma PD}$, and $\boldsymbol{\Sigma}_{\Gamma adapter}$, respectively. If there is no correlation between the covariances, they can be propagated to the covariance of the impedance mismatch $\boldsymbol{\Sigma}_{mismatch}$ as follows:

$$\begin{aligned}\boldsymbol{\Sigma}_{mismatch} = \mathbf{J}_{\Gamma scope}\boldsymbol{\Sigma}_{\Gamma scope}\mathbf{J}'_{\Gamma_{scope}} + \mathbf{J}_{\Gamma PD}\Sigma_{\Gamma PD}\mathbf{J}'_{\Gamma PD} \\ + \mathbf{J}_{\Gamma adapter}\boldsymbol{\Sigma}_{\Gamma adapter}\mathbf{J}'_{\Gamma_{adapter}}\end{aligned} \tag{14}$$

where $\mathbf{J}_{\Gamma scope}$, $\mathbf{J}_{\Gamma PD}$, and $\mathbf{J}_{\Gamma \mathrm{adapter}}$ have the same numerators as in (13), and the denominators are replaced with $\partial\Gamma_{scope}(f_k)$, $\partial\Gamma_{PD}(f_k)$, and $\partial S_{xx}(f_k)$, respectively. Therefore, $\mathbf{J}_{\Gamma scope}$ and $\mathbf{J}_{\Gamma PD}$ have a size of $2M \times 2M$, and $\mathbf{J}_{\Gamma adapter}$ has a size of $2\,\mathrm{M} \times 8\,M$.

$$\mathbf{J}_{\Gamma scope} = \begin{bmatrix} \dfrac{\partial |H(f_0)|}{\partial \Re(\Gamma_{scope}(f_0))} & \cdots & \dfrac{\partial |H(f_0)|}{\partial \Im\left(\Gamma_{scope}(f_M)\right)} \\ \vdots & \ddots & \vdots \\ \dfrac{\partial \arg\left(H(f_M)\right)}{\partial \Re(\Gamma_{scope}(f_0))} & \cdots & \dfrac{\partial \arg\left(H(f_M)\right)}{\partial \Im\left(\Gamma_{scope}(f_M)\right)} \end{bmatrix}$$

$$\mathbf{J}_{\Gamma PD} = \begin{bmatrix} \dfrac{\partial |H(f_0)|}{\partial \Re(\Gamma_{PD}(f_0))} & \cdots & \dfrac{\partial |H(f_0)|}{\partial \Im\left(\Gamma_{PD}(f_M)\right)} \\ \vdots & \ddots & \vdots \\ \dfrac{\partial \arg\left(H(f_M)\right)}{\partial \Re\left(\Gamma_{PD}(f_0)\right)} & \cdots & \dfrac{\partial \arg\left(H(f_M)\right)}{\partial \Im\left(\Gamma_{PD}(f_M)\right)} \end{bmatrix}$$

$$\mathbf{J}_{\Gamma adapter} == \begin{bmatrix} \dfrac{\partial |H(f_0)|}{\partial \Re |S_{11}(f_0)|} & \cdots & \dfrac{\partial \arg\left(H(f_M)\right)}{\partial \Re |S_{11}(f_0)|} \\ \dfrac{\partial |H(f_0)|}{\partial \Re |S_{21}(f_0)|} & \cdots & \dfrac{\partial \arg\left(H(f_M)\right)}{\partial \Re |S_{21}(f_0)|} \\ \dfrac{\partial |H(f_0)|}{\partial \Re |S_{12}(f_0)|} & \cdots & \dfrac{\partial \arg\left(H(f_M)\right)}{\partial \Re |S_{12}(f_0)|} \\ \dfrac{\partial |H(f_0)|}{\partial \Re |S_{22}(f_0)|} & \cdots & \dfrac{\partial \arg\left(H(f_M)\right)}{\partial \Re |S_{22}(f_0)|} \\ \vdots & & \vdots \\ \dfrac{\partial |H(f_0)|}{\partial \Im |S_{11}(f_M)|} & \cdots & \dfrac{\partial \arg\left(H(f_M)\right)}{\partial \Im |S_{11}(f_M)|} \\ \dfrac{\partial |H(f_0)|}{\partial \Im |S_{21}(f_M)|} & \cdots & \dfrac{\partial \arg\left(H(f_M)\right)}{\partial \Im |S_{21}(f_M)|} \\ \dfrac{\partial |H(f_0)|}{\partial \Im |S_{12}(f_M)|} & \cdots & \dfrac{\partial \arg\left(H(f_M)\right)}{\partial \Im |S_{12}(f_M)|} \\ \dfrac{\partial |H(f_0)|}{\partial \Im |S_{22}(f_M)|} & \cdots & \dfrac{\partial \arg\left(H(f_M)\right)}{\partial \Im |S_{22}(f_M)|} \end{bmatrix}'$$

where $\Re(\cdot)$, and $\Im(\cdot)$ represent real and imaginary numbers of arguments, respectively. Note that covariance $\boldsymbol{\Sigma}_{\Gamma scope}$, $\boldsymbol{\Sigma}_{\Gamma PD}$, and $\boldsymbol{\Sigma}_{\Gamma adapter}$ for the complex values Γ_{scope}, Γ_{PD}, and S_{xx} consist of the following:

$$\Sigma = \begin{bmatrix} \Sigma_{RR} & \Sigma_{RI} \\ \Sigma_{IR} & \Sigma_{II} \end{bmatrix}$$

where the subscripts R and I represent a real number and an imaginary number, respectively.

The covariance $\boldsymbol{\Sigma}_{\mathrm{V}\_PD}$ for the voltage response of the calibrated PD was provided from NIST and should be counted in the uncertainty analysis. Similarly, the $\boldsymbol{\Sigma}_{\mathrm{V}\_PD}$ also propagated to the covariance of the frequency response $\boldsymbol{\Sigma}_{PD}$.

$$\boldsymbol{\Sigma}_{PD} = \mathbf{J}_{PD}\boldsymbol{\Sigma}_{V\_PD}\mathbf{J}'_{PD} \tag{15}$$

The Jacobian matrix $\mathbf{J}_{PD}$ is also the same as the numerators in (13) and the denominators are replaced with $\partial \mathrm{V}_{PD}(f_k)$.

$$\mathbf{J}_{PD} = \begin{bmatrix} \frac{\partial\,|H(f_0)|}{\partial \Re\,(V_{PD}(f_0))} & \cdots & \frac{\partial\,|H(f_0)|}{\partial \Im\,(V_{PD}(f_M))} \\ \vdots & \ddots & \vdots \\ \frac{\partial\,\arg\,(H(f_M))}{\partial \Re\,(V_{PD}(f_0))} & \cdots & \frac{\partial\,\arg\,(H(f_M))}{\partial \Im\,(V_{PD}(f_M))} \end{bmatrix}$$

Fig. 5 shows the standard deviations calculated from (12), (14) and (15). The standard deviation for the impedance mismatch (dash-dotted line) gradually increases as the frequency increases, while the standard deviation for the measurement pulse (solid line) is almost constant because the variance, which is caused by independent random jitter and noise, is relatively larger than the variance due to alignment, as described above. The standard deviation of the pulse, however, greatly increases when the frequency is above 25 GHz because the measured H value decreases by about 4 to 5 dB in this frequency region. As a result, the covariance for the pulse relatively increases compared to other frequency regions.

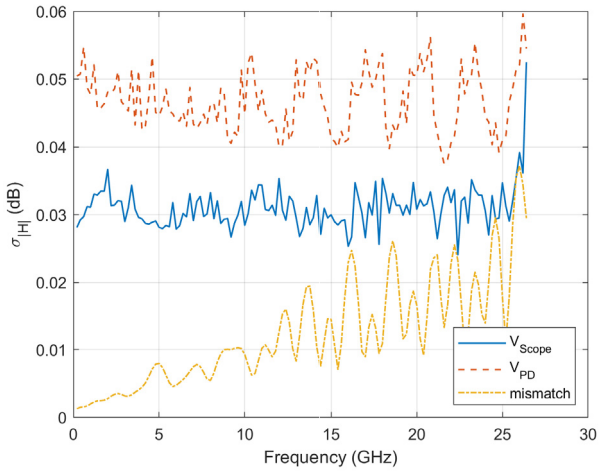

FIGURE 5. Contribution of the measurement error on the uncertainty.

C. REPRODUCIBILITY

To obtain the reproducibility of the measurement, the frequency response of the RTDO during testing was measured three times. In each measurement, all instruments, components, and cables were disconnected and reconnected. The reproducibility $\mathbf{\Sigma}_{reprod}$ was calculated by dividing the covariance of these measurements by the number of measurements n.

D. 95% CONFIDENCE INTERVAL

Finally, the covariance of the frequency response including the reproducibility was as follows.

$$\mathbf{\Sigma}_{total} = \mathbf{\Sigma}_{scope} + \mathbf{\Sigma}_{PD} + \mathbf{\Sigma}_{mismatch} + \mathbf{\Sigma}_{reprod}$$

The standard deviation was then be obtained by taking the square root of the diagonal matrix from the covariance matrix S_{total}. Fig. 6 shows the 95% confidence interval calculated by multiplying the coverage factor $k = 2$ in terms of amplitude and phase, respectively. The phase is detrended by subtracting the linear phase to have a small rms value up to 25 GHz. The 95% confidence interval for the magnitude is about 0.2 dB, and the phase is about 3 degrees. The swept sine method is also plotted in Fig. 6(a) to compare it with the proposed method. The swept sine method measures the response of the oscilloscope based on the power meter, which is directly traceable to the RF power standard [14]. The proposed method agrees well with the swept sine method within its uncertainties.

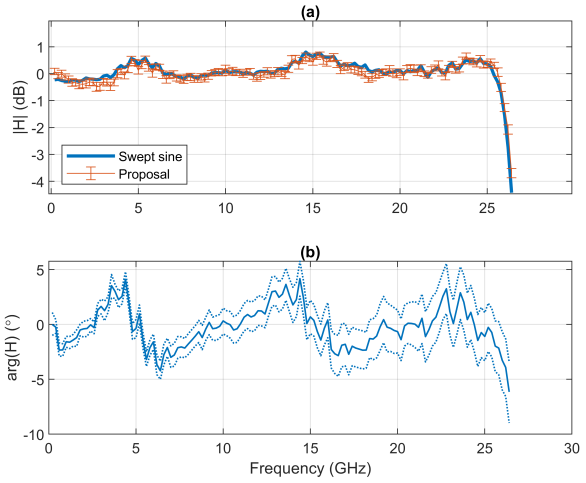

FIGURE 6. Measurement uncertainty of the frequency response of a single ADC (a) amplitude (b) detrended phase.

IV. CONCLUSION

In this paper, we described a characterization method for the frequency response of individual ADCs in commercial RTDOs using a calibrated pulse. We acquired the covariance of the frequency response by analyzing the uncertainties of RTDO measurement, impedance mismatch correction, pulse standard, and reproducibility. The standard deviation was easily obtained by taking the square root of the diagonal matrix from the covariance matrix. The 95% confidence interval had an amplitude uncertainty of about 0.2 dB and a phase uncertainty of about 3°. We also compared the proposed method with the swept sine method and confirmed that they agree well within its uncertainties.

REFERENCES

[1] W. C. Black and D. A. Hodges, "Time interleaved converter arrays," *IEEE J. Solid-State Circuits*, vol. 15, no. 6, pp. 1022–1029, Dec. 1980.

[2] C. Cho, J.-G. Lee, P. D. Hale, J. A. Jargon, P. Jeavons, J. Schlager, and A. Dienstfrey, "Calibration of channel mismatch in time-interleaved real-time digital oscilloscopes," in *Proc. 85th Microw. Meas. Conf. (ARFTG)*, May 2015, pp. 1–5.

[3] C. Cho, J. G. Lee, P. D. Hale, J. A. Jargon, P. Jeavons, J. Schlager, and A. Dienstfrey, "Calibration of time-interleaved errors in digital real-time oscilloscopes," *IEEE Trans. Microw. Theory Techn.*, vol. 64, no. 11, pp. 4071–4079, Nov. 2016.

[4] D. Kim, J.-G. Lee, D.-J. Lee, and C. Cho, "Traceable calibration for a digital real-time oscilloscope with time interleaving architecture," *Meas. Sci. Technol.*, vol. 29, no. 1, Jan. 2018, Art. no. 015003.
[5] C. Cho, D.-J. Lee, H. Koo, and J.-G. Lee, "Frequency response of real-time digital oscilloscope with time-interleaving architecture," in *Proc. 93rd ARFTG Microw.*, Jun. 2019, pp. 1–4.
[6] C. Cho, J.-G. Lee, J.-H. Kim, and D.-C. Kim, "Uncertainty analysis in EVM measurement using a Monte Carlo simulation," *IEEE Trans. Instrum. Meas.*, vol. 64, no. 6, pp. 1413–1418, Jun. 2015.
[7] D. F. Williams, T. S. Clement, P. D. Hale, and A. Dienstfrey, "Terminology for high-speed sampling-oscilloscope calibration," in *Proc. 68th ARFTG Microw., Meas.*, Nov./Dec. 2006, pp. 1–6.
[8] J. A. Jargon, C. Cho, D. F. Williams, and P. D. Hale, "Physical models for 2.4 mm and 3.5 mm coaxial VNA calibration kits developed within the NIST microwave uncertainty framework," in *Proc. 85th ARFTG Microw., Meas.*, May 2015, pp. 1–7.
[9] C. Cho, J.-S. Kang, J.-G. Lee, and H. Koo, "Characterization of a 1 mm (DC to 110 GHz) calibration kit," *J. Electromagn. Eng. Sci.*, vol. 19, no. 4, pp. 272–278, Oct. 2019.
[10] A. Lewandowski, D. F. Williams, P. D. Hale, J. C. M. Wang, and A. Dienstfrey, "Covariance-based vector-network-analyzer uncertainty analysis for time- and frequency-domain measurements," *IEEE Trans. Microw. Theory Techn.*, vol. 58, no. 7, pp. 1877–1886, Jul. 2010.
[11] S. van de Geer, "Least squares estimation," in *Encyclopedia of Statistics in Behavioral Science*. Hoboken, NJ, USA: Wiley, 2005.
[12] *Evaluation of Measurement Data-Guide to the Expression of Uncertainty in Measurement, Joint Committee for Guides in Metrology*, document JCGM 100, 2008.
[13] D. F. Williams, A. Lewandowski, T. S. Clement, J. C. M. Wang, P. D. Hale, J. M. Morgan, D. A. Keenan, and A. Dienstfrey, "Covariance-based uncertainty analysis of the NIST electrooptic sampling system," *IEEE Trans. Microw. Theory Tech.*, vol. 54, no. 1, pp. 481–490, Jan. 2006.
[14] A. Dienstfrey, P. D. Hale, D. A. Keenan, T. S. Clement, and D. F. Williams, "Minimum-phase calibration of sampling oscilloscopes," *IEEE Trans. Microw. Theory Techn.*, vol. 54, no. 8, pp. 3197–3208, Aug. 2006.

CHIHYUN CHO received the B.S., M.S., and Ph.D. degrees in electronic and electrical engineering from Hongik University, Seoul, South Korea, in 2004, 2006, and 2009, respectively. From 2009 to 2012, he participated in the development of military communication systems at the Communication Research and Development Center, Samsung Thales, Seongnam, South Korea. Since 2012, he has been with the Korea Research Institute of Standards and Science (KRISS), Daejeon, South Korea. In 2014, he was a Guest Researcher with the National Institute of Standards and Technology (NIST), Boulder, CO, USA. His current research interests include microwave metrology, time-domain measurement, and standard of communication parameters. He served on the Presidential Advisory Council on Science and Technology (PACST), Seoul, from 2016 to 2017.

HYUNJI KOO received the B.S. and Ph.D. degrees in electrical engineering from the Korea Advanced Institute of Science and Technology (KAIST), Daejeon, South Korea, in 2008 and 2015, respectively. From March 2015 to August 2015, she was a Postdoctoral Research Fellow with the School of Electrical Engineering, KAIST. Since September 2015, she has been a Senior Research Scientist with the Center for Electromagnetic Standards, Korea Research Institute of Standards and Science (KRISS), Daejeon. In 2018, she was a Visiting Researcher with the National Physical Laboratory (NPL), Teddington, U.K. Her current research interest includes the characterization of on-wafer or PCB devices.

JAE-YONG KWON (SM'17) received the B.S. degree in electronics from Kyungpook National University, Daegu, South Korea, in 1995, and the M.S. and Ph.D. degrees in electrical engineering from the Korea Advanced Institute of Science and Technology, Daejeon, South Korea, in 1998 and 2002, respectively. He was a Visiting Scientist with the Department of High-Frequency and Semiconductor System Technologies, Technical University of Berlin, Berlin, Germany, in 2001, and the National Institute of Standards and Technology, Boulder, CO, USA, in 2010. From 2002 to 2005, he was a Senior Research Engineer with the Devices and Materials Laboratory, LG Electronics Institute of Technology, Seoul, South Korea. Since 2005, he has been a Principal Research Scientist with the Division of Physical Metrology, Center for Electromagnetic Metrology, Korea Research Institute of Standards and Science, Daejeon. Since 2013, he has been a Professor of science of measurement with the University of Science and Technology, Daejeon. His current research interests include electromagnetic power, impedance, and antenna measurement.

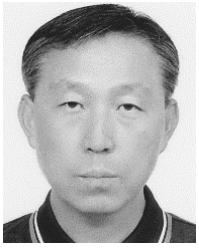

JOO-GWANG LEE (M'97) was born in Seoul, South Korea, in 1960. He received the B.S. degree in electronic engineering from Hanyang University, Seoul, in 1984, and the M.S. and Ph.D. degrees from the Korea Advanced Institute of Science and Technology, Daejeon, South Korea, in 1994 and 2000, respectively. Since 1986, he has been with the Korea Research Institute of Standards and Science, Daejeon. His current research interests include radio-frequency and microwave measurements, time-domain metrology, and electromagnetic compatibility.